

Ternary iron selenide $K_{0.8}Fe_{1.6}Se_2$ is an antiferromagnetic semiconductor

Xun-Wang Yan^{1,2}, Miao Gao¹, Zhong-Yi Lu^{1,*} and Tao Xiang^{2,3†}

¹*Department of Physics, Renmin University of China, Beijing 100872, China*

²*Institute of Theoretical Physics, Chinese Academy of Sciences, Beijing 100190, China and*

³*Institute of Physics, Chinese Academy of Sciences, Beijing 100190, China*

(Dated: October 23, 2018)

We have studied electronic and magnetic structures of $K_{0.8+x}Fe_{1.6}Se_2$ by performing the first-principles electronic structure calculations. The ground state of the Fe-vacancies ordered $K_{0.8}Fe_{1.6}Se_2$ is found to be a quasi-two-dimensional blocked checkerboard antiferromagnetic (AFM) semiconductor with an energy gap of 594 meV and a large ordering magnetic moment of $3.37 \mu_B$ for each Fe atom, in excellent agreement with the neutron scattering measurement. The underlying mechanism is the chemical-bonding-driven tetramer lattice distortion. $K_{0.8+x}Fe_{1.6}Se_2$ with finite x is a doped AFM semiconductor with low conducting carrier concentration which is approximately proportional to the excess potassium content, consistent qualitatively with the infrared observation. Our study reveals the importance of the interplay between antiferromagnetism and superconductivity in these materials. This suggests that $K_{0.8}Fe_{1.6}Se_2$, instead of KFe_2Se_2 , should be regarded as a parent compound from which the superconductivity emerges upon electron or hole doping.

PACS numbers: 74.70.Xa, 74.20.Pq, 74.20.Mn

The recent discovery of high- T_c superconductivity in potassium intercalated FeSe[1] and other iron-based chalcogenides[2, 3] has triggered a surge of interest for the investigation of unconventional superconducting pairing mechanism. In particular, it was found that the superconductivity in these materials coexists with a strong antiferromagnetic (AFM) order with an unprecedentedly large magnetic moment of $3.31 \mu_B/Fe$ formed below a Neel temperature of $559K$ [4, 5], meanwhile the conducting electron concentration is extremely low[6]. Unlike the collinear [7–9] or bi-collinear[10–12] AFM order observed in the parent compounds of other iron-based superconductors, the neutron observation found that these materials have a blocked checkerboard AFM order[5].

These compounds have the $ThCr_2Si_2$ type crystal structure, as shown in Fig. 1(a), isostructural with 122-type iron pnictides [13]. From the latest X-rays, transmission electron microscopy, and neutron scattering measurements, it was suggested that the composition of the K-intercalated FeSe superconductors $K_yFe_{2-x}Se_2$ is close to $K_yFe_{1.6}Se_2$ with a fivefold expansion of the parent $ThCr_2Si_2$ unit cell in the ab plane, namely a $\sqrt{5} \times \sqrt{5}$ Fe-vacancies superstructure [5, 14], which corresponds to one-fifth Fe-vacancies. In an Fe-Fe square lattice, an Fe atom nearby a vacancy is 3-Fe-neighbored, or 2-Fe-neighbored, or even 1-Fe-neighbored. Topologically a square lattice composed only by 3-Fe-neighbored Fe atoms exists only in one arranging order but with two different kinds of chirality, right-handed or left-handed rotations[15], as shown in Fig. 1(b) and (c), respectively. This is exactly a $\sqrt{5} \times \sqrt{5}$ superstructure.

The peculiar properties observed in K-intercalated iron-based chalcogenide superconductors indicate that these materials represent a special limit where the interplay between antiferromagnetism and superconductivity plays an important role in the formation of supercon-

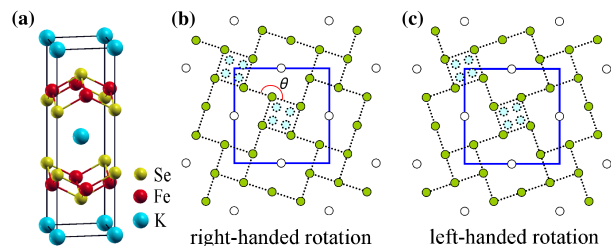


FIG. 1: (Color online) $K_yFe_xSe_2$ with the $ThCr_2Si_2$ -type structure: (a) a tetragonal unit cell containing two formula units without any vacancy; (b) and (c) are schematic top view of an Fe-Fe square layer with one-fifth Fe-vacancies ($x = 1.6$) ordered with the right- and left-chirality, respectively. In this $\sqrt{5} \times \sqrt{5}$ lattice, each Fe is coordinated with 3 neighboring Fe atoms. The squares enclosed by the solid lines denote the unit cells. The filled circles denote the Fe atoms while the empty circles denote the Fe-vacancies. After optimizing the structure by the energy minimization, the Fe atoms go into a blocked distribution from a uniform square distribution, in which the four closest Fe atoms form a block, represented by dashed (blue) circles in (b) and (c), whose bond distance is shorter than that of the uniform Fe square lattice (green dots). Correspondingly, the angle θ decreases from 180° to $176^\circ - 178^\circ$.

ducting pairs. To reveal the hidden physics, we have performed the first-principles electronic structure calculations for $K_{0.8+x}Fe_{1.6}Se_2$ with $x = 0$ and ± 0.1 . We find that the ground state of $K_{0.8}Fe_{1.6}Se_2$ is an AFM semiconductor with a blocked checkerboard long-range AFM order (Fig. 3(c)) and an energy gap of 594 meV, and $K_{0.8\pm 0.1}Fe_{1.6}Se_2$ are doped electron- or hole-type AFM semiconductors. $K_{0.8}Fe_{1.6}Se_2$ is thus an essential parent compound so that the observed superconductivity in $K_yFe_{2-x}Se_2$ is based on the doped AFM semiconductors.

In our calculations the plane wave basis method was

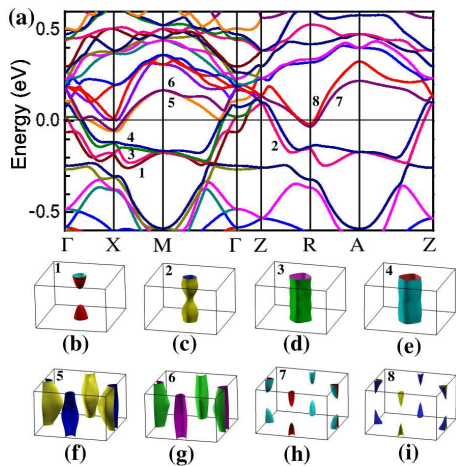


FIG. 2: (Color online) Electronic structure of $\text{K}_{0.8}\text{Fe}_{1.6}\text{Se}_2$ with one-fifth Fe-vacancies ordered in a way as shown by Fig. 1(b) or (c) in the nonmagnetic state: (a) the band structure; (b-i) are the Fermi surface sheets due to the bands crossing the Fermi energy denoted by (1-8) in (a), respectively. The corresponding Brillouin zone is shown in Fig. 4(b). The Fermi energy sets to zero.

used. We adopted the generalized gradient approximation (GGA) with Perdew-Burke-Ernzerhof formula [16] for the exchange-correlation potentials. The ultrasoft pseudopotentials [17] were used to model the electron-ion interactions. The kinetic energy cut-off and the charge density cut-off of the plane wave basis were chosen to be 800 eV and 6400 eV, respectively. A mesh of $18 \times 18 \times 8$ k-points were sampled for the Brillouin-zone integration while the Gaussian broadening technique was used in the case of metallic states. In the calculations, the lattice parameters with the internal atomic coordinates were optimized by the energy minimization. The optimized tetragonal lattice parameters in the magnetic states agree excellently with the experimental data[5].

In the calculations, we adopted a $\sqrt{5} \times \sqrt{5} \times 1$ tetragonal supercell, in which there are two FeSe layers with total 16 Fe atoms and 4 Fe-vacancies, 20 Se atoms, and 8 K atoms and 2 K-vacancies, to represent $\text{K}_{0.8}\text{Fe}_{1.6}\text{Se}_2$. For K atoms, there are two inequivalent positions in the supercell. Accordingly, there are a number of inequivalent arrangements for the two K-vacancies. From the calculations, we find that both the electronic band structures and the Fe moments are hardly affected by these inequivalent arrangements. And the energy difference among these different K arrangements is within 1 meV/Fe in both spin-polarized and spin-unpolarized cases. This is consistent with the experimental observation that the vacancies on K sites are in positional disorder [14].

Figure 2 shows the non-magnetic band structure and Fermi surface of $\text{K}_{0.8}\text{Fe}_{1.6}\text{Se}_2$ with one-fifth Fe-vacancies ordered in a way as shown by Fig. 1(b) or (c). There are 8 bands crossing the Fermi level. An important feature

revealed by the calculation is that due to a substantial lattice distortion driven by Fe vacancies, the bond distances among four closest Fe atoms around a Se atom are reduced. These four Fe atoms will form a compact square (we will call it a block below), as shown by the light blue circles in Fig. 1(b). The angle θ , which is shown in Fig. 1(b), decreases from 180° to about 176° . As a result, the Fe-Fe and Fe-Se chemical bonds within each block become stronger. This gains an energy of about 160 meV/Fe. Such a tetramer lattice distortion is not due to the spin-phonon interaction since it happens in both non-magnetic and magnetic states. It is in fact driven by the chemical bonding, namely this is a chemical-bonding-driven lattice distortion. On the contrary, all the structural or lattice distortions previously found in the iron-pnictides and chalcogenides are driven by the spin-phonon interactions [8], namely magnetism-driven lattice distortions.

Figure 3 shows eight possibly energetically favored magnetic orders arranged in a right-chirality lattice (Fig. 1(b)). From the calculations, if the energy of the non-magnetic state is set to zero, we find that the respective energies of these eight states, i.e. the ferromagnetic, checkerboard AFM, blocked checkerboard AFM, quaternary collinear AFM, collinear AFM, bi-collinear AFM, cell-in collinear AFM, and cell-in bi-collinear AFM states, are (-0.070, -0.189, -0.342, -0.232, -0.293, -0.229, -0.254, -0.267) eV/Fe for $\text{K}_{0.8}\text{Fe}_{1.6}\text{Se}_2$. The corresponding magnetic moments are (3.29, 2.76, 3.37, 3.10, 3.32, 3.22, 3.20, 3.26) μ_B/Fe . The ground state of $\text{K}_{0.8}\text{Fe}_{1.6}\text{Se}_2$ is thus found to have a blocked checkerboard AFM order (Fig. 3(c)) with a large magnetic moment of 3.37 μ_B/Fe , in agreement excellently with the latest neutron scattering measurement [5]. The similar magnetic order was also reported in a calculation to show metallic $\text{KFe}_{1.6}\text{Se}_2$ [18].

Here we emphasize that it is the chemical-bonding driven tetramer lattice distortion mentioned above that makes the blocked checkerboard AFM order be the lowest in energy. Without this tetramer lattice distortion, the energy of the collinear AFM state (Fig. 3(e)) is in fact 43 meV/Fe lower than that of the blocked checkerboard AFM state. The collinear AFM order is the ground state magnetic order of the iron-pnictides, driven by the As-bridged AFM superexchange interaction between two next-nearest Fe atoms, which dominates over other exchange interactions. However, in $\text{K}_{0.8}\text{Fe}_{1.6}\text{Se}_2$, the chemical-bonding driven tetramer lattice distortion reduces the bond distance within each block so that the ferromagnetic exchange interaction between the two nearest Fe atoms inside a block and the AFM exchange interactions between neighboring two blocks are substantially enhanced. It turns out that the blocked checkerboard AFM order dominates over all the other magnetic orders.

Figure 4(a) shows the electronic band structure of $\text{K}_{0.8}\text{Fe}_{1.6}\text{Se}_2$ in the blocked checkerboard AFM ground state. To our surprise, we find that the compound

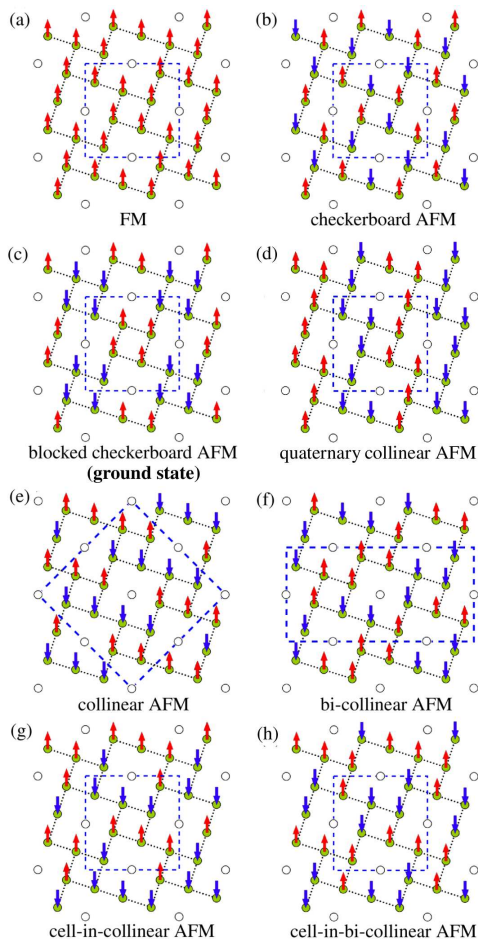


FIG. 3: (Color online) Schematic top view of eight possible magnetic orders in the Fe-Fe square layer with one-fifth Fe-vacancies. Among these magnetic orders, the blocked checkerboard antiferromagnetic order in (c) is the ground state, in which the magnetic moments within each block are in parallel, but the magnetic moments for the neighboring two blocks are in anti-parallel. The Fe spins are shown by arrows. The empty circles mark the Fe vacancies. The squares or rectangles enclosed by the dashed lines denote the magnetic unit cells.

$\text{K}_{0.8}\text{Fe}_{1.6}\text{Se}_2$ is an AFM semiconductor with an energy band gap as large as ~ 594 meV. This is different from the parent compounds of other iron-based superconductors, they are either magnetic or non-magnetic semimetals. $\text{K}_{0.8}\text{Fe}_{1.6}\text{Se}_2$ with the checkerboard AFM, collinear AFM, or quaternary collinear AFM order is also found to be semiconducting. The corresponding energy band gaps are 22, 73, and 185 meV, respectively. With any other magnetic order, $\text{K}_{0.8}\text{Fe}_{1.6}\text{Se}_2$ is in a metallic state.

Figure 5(a) shows the total and orbital-resolved partial density of states (spin-up part) for $\text{K}_{0.8}\text{Fe}_{1.6}\text{Se}_2$ in the blocked checkerboard AFM ground state. We find that the states around the top valence bands are composed of both Fe-3d and Se-4p orbitals with the same peak energies. This is consistent with the localized fea-

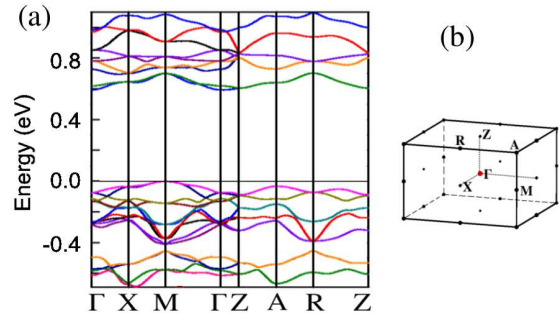


FIG. 4: (Color online) (a) Electronic band structure of Fe-vacancies ordered $\text{K}_{0.8}\text{Fe}_{1.6}\text{Se}_2$ in the ground state with a blocked checkerboard antiferromagnetic order (Fig. 3(c)). (b) Brillouin zone. Here the top of the valence band is set to zero.

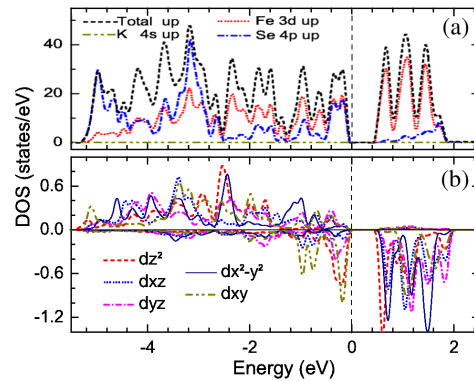


FIG. 5: (Color online) $\text{K}_{0.8}\text{Fe}_{1.6}\text{Se}_2$ in the blocked checkerboard antiferromagnetic ground state: (a) total and orbital-resolved partial density of states (spin-up part); (b) projected density of states onto the five Fe-3d orbitals at an Fe atom. Here the top of the valence band sets to zero. And x -axis is along the two next-nearest neighbor Fe-Fe.

tures of these bands, enhanced by Fe-Fe and Fe-Se chemical bonding due to the tetramer lattice distortion. On the contrary, the lower conduction bands are mainly contributed by the Fe-3d orbitals.

By projecting the density of states onto the five 3d orbitals of an Fe atom in the blocked checkerboard AFM ground state (Fig. 5(b)), we find that the five up-spin orbitals are almost fully filled. This suggests that the crystal field splitting induced by Se atoms is small, similar to the case of iron-pnictides [8]. The large magnetic moment formed around each Fe results from the Hund's rule coupling. The down spin orbitals are partially filled by d_{z^2} , d_{xy} , and d_{yz} orbitals. Such anisotropy among the five down spin orbitals in $\text{K}_{0.8}\text{Fe}_{1.6}\text{Se}_2$ is enhanced by the ordered Fe-vacancies.

We have verified the above results using the virtual crystal approximation (VCA) for K atoms. We then replaced $\text{K}_{0.8}$ by $\text{K}_{0.7}$ and $\text{K}_{0.9}$ respectively by using VCA to simulate the hole-doping and electron-doping effect upon the AFM semiconductor $\text{K}_{0.8}\text{Fe}_{1.6}\text{Se}_2$. As shown

in Fig. 6, the electronic band structure of hole or electron doped $K_{0.8\pm 0.1}Fe_{1.6}Se_2$ is almost the same as the one for the un-doped case (Fig. 4). The magnetic moments of Fe ions are also hardly changed by doping. The doped electrons and holes occupy the bottom conduction bands and the top valence bands, respectively. The volumes enclosed by the Fermi surfaces are found to be 0.529 holes/cell and 0.642 electrons/cell, namely 5.00×10^{20} holes/ cm^3 and 6.06×10^{20} electrons/ cm^3 , respectively. In principle, every excess $K_{0.1}$ can supply 1 electron/cell to the material. Thus both electron and hole doping upon $K_{0.8}Fe_{1.6}Se_2$ are very efficient, similar to conventional semiconductors. But the total carrier concentration is very low, in comparison with other iron-based superconductors. This agrees with the infrared measurement[6].

We have calculated the formation energy of $K_{0.8+x}Fe_{1.6-x/2}Se_2$, defined by $(0.8+x)E_K + (1.6-x/2)E_{Fe} + 2E_{Se} - E_x$, where E_K , E_{Fe} , and E_{Se} are the atomic energies of K, Fe, and Se, respectively, and E_x is the total energy of $K_{0.8+x}Fe_{1.6-x/2}Se_2$. For $x = 0, 0.2$ and -0.4 , corresponding to $K_{0.8}Fe_{1.6}Se_2$, $KFe_{1.5}Se_2$, and $K_{0.4}Fe_{1.8}Se_2$, we find that the formation energies are 16.652, 16.564, and 16.632 eV, respectively. Here these stoichiometric compounds are in a balance of chemical valence, in which K, Fe and Se are in 1+, 2+, and 2- valence states, respectively. The ground states of Fe-vacancies ordered $K_{0.4}Fe_{1.8}Se_2$ and $KFe_{1.5}Se_2$ are in a collinear AFM order[9]. The formation energy data indicate that $K_{0.8}Fe_{1.6}Se_2$ is energetically more favorable when K atoms are intercalated into FeSe. Thus $K_{0.8}Fe_{1.6}Se_2$ is more likely to be the parent compound of potassium intercalated FeSe superconductors upon doping. The superstructure $\sqrt{5} \times \sqrt{5}$ with $Fe_{1.6}Se_2$ layers may thus be the framework or backbone of superconductors $K_yFe_{2-x}Se_2$.

We have also calculated the electronic structures of $A_{0.8}Fe_{1.6}Se_2$ (A=Rb, Cs, or Tl) and found that they are all AFM semiconductors. The energy band gaps of these compounds are 571, 548, and 440 meV, respectively.

In conclusion, we have performed the first principles calculations for the electronic structure and magnetic order of $K_yFe_{2-x}Se_2$. We find that the ground state of $K_{0.8}Fe_{1.6}Se_2$ is a quasi-two-dimensional antiferromagnetic semiconductor with an energy gap of 594 meV. The ground state magnetic order is a blocked checkerboard antiferromagnetic order with a large magnetic moment of $3.37\mu_B$, in agreement with the experimental measurements. The underlying mechanism is the chemical-bonding-driven tetramer lattice distortion. Doping electrons or holes into $K_{0.8}Fe_{1.6}Se_2$ by intercalating more or less K to the compound almost do not change the band structure as well as the blocked checkerboard antiferromagnetic order. Our result suggests that $K_{0.8}Fe_{1.6}Se_2$ serves as a parent compound which becomes superconducting upon electron or hole doping.

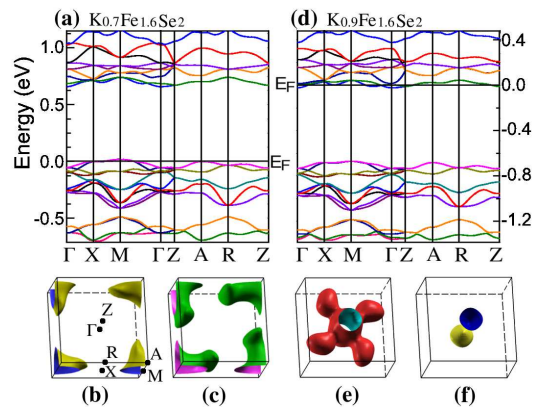


FIG. 6: (Color online) Electronic band structures and Fermi surfaces in the blocked checkerboard antiferromagnetic ground state with the left chirality: (a-c) for $K_{0.7}Fe_{1.6}Se_2$ and (d-f) for $K_{0.9}Fe_{1.6}Se_2$, to represent the hole-doping or electron-doping upon $K_{0.8}Fe_{1.6}Se_2$, respectively. The Fermi energy sets to zero.

We would like to thank W. Bao for helpful discussion and P.C. Dai for drawing our attention for the magnetic ordered state as shown in Fig. 3(d). This work is partially supported by National Natural Science Foundation of China and by National Program for Basic Research of MOST, China.

* Electronic address: zlu@ruc.edu.cn

† Electronic address: txiang@iphy.ac.cn

- [1] J. Guo, *et al.*, Phys. Rev. B **82**, 180520(R) (2010).
- [2] A. Krzton-Maziopa, *et al.*, arXiv:1012.3637.
- [3] M. Fang, *et al.*, arXiv:1012.5236.
- [4] Z. Shermadini *et al.*, arXiv:1101.1873, accepted by PRL (2011)
- [5] W. Bao, *et al.*, arXiv:1102.0830.
- [6] R.H. Yuan, T. Dong, G.F. Chen, J.B. He, D.M. Wang, and N. L. Wang, arXiv:1102.1381 (unpublished).
- [7] C. de la Cruz *et al.*, Nature (London) **453**, 899 (2008).
- [8] F. Ma, Z.Y. Lu, and T. Xiang, Phys. Rev. B **78**, 224517 (2008); Front. Phys. China, **5**(2), 150 (2009).
- [9] X.W. Yan, M. Gao, Z.Y. Lu, and T. Xiang, Phys. Rev. Lett. **106**, 087005 (2011).
- [10] F. Ma *et al.*, Phys. Rev. Lett. **102**, 177003 (2009).
- [11] W. Bao *et al.*, Phys. Rev. Lett. **102**, 247001 (2009).
- [12] S.L. Li *et al.*, Phys. Rev. B **79**, 054503 (2009).
- [13] M. Rotter, M. Tegel, and D. Johrendt, Phys. Rev. Lett. **101**, 107006 (2008).
- [14] J. Bacsá, *et al.*, arXiv:1102.0488.
- [15] H. Sabrowsky, *et al.*, J. Magn. Magn. Mater. **54-57**, 1497-1498 (1986).
- [16] J. P. Perdew, K. Burke, and M. Ernzerhof, Phys. Rev. Lett. **77**, 3865 (1996).
- [17] D. Vanderbilt, Phys. Rev. B **41**, 7892 (1990).
- [18] C. Cao and J. Dai, arXiv:1102.1344.